

## Critical Behavior and Scaling in Vacuum Axisymmetric Gravitational Collapse

Andrew M. Abrahams<sup>(a)</sup>

*Center for Radiophysics and Space Research, Cornell University, Ithaca, New York 14853*

Charles R. Evans

*Department of Physics and Astronomy, University of North Carolina, Chapel Hill, North Carolina 27599*

(Received 22 December 1992)

We report a second example of critical behavior in gravitational collapse. Collapse of axisymmetric gravitational wave packets is computed numerically for a one-parameter family of initial data. A black hole first appears along the sequence at a critical parameter value  $p^*$ . As with spherical scalar-field collapse, a power law is found to relate black-hole mass (the order parameter) and critical separation:  $M_{\text{BH}} \propto |p - p^*|^\beta$ . The critical exponent is  $\beta \simeq 0.37$ , remarkably close to that observed by Choptuik. Near-critical evolutions produce echoes from the strong-field region which appear to exhibit scaling.

PACS numbers: 04.20.Jb, 02.60.Cb, 04.30.+x, 97.60.Lf

Critical phenomena have recently been discovered in classical general relativity. Using a sensitive, adaptive-mesh-refinement scheme, Choptuik [1] has studied spherically symmetric gravitational collapse of a massless scalar field  $\phi(r, t)$ . One-parameter families of solutions  $\mathcal{S}_k[p]$  are numerically computed, with each family  $k$  generated by evolving Cauchy data of initially ingoing wave packets, or shells, of scalar field. The parameter  $p$  characterizes the strength of the ensuing gravitational self-interaction of the wave packet. For each family, there exists along the sequence a critical parameter value  $p^*$  that separates supercritical solutions  $\mathcal{S}[p > p^*]$ , which contain black holes, from subcritical solutions  $\mathcal{S}[p < p^*]$ , which do not (assuming an orientation for  $p$ ). Critical behavior is exhibited in solutions as  $p \rightarrow p^*$ . For  $p > p^*$  and as  $p \rightarrow p^*$  black-hole mass is found to have a power-law dependence on critical separation:  $M_{\text{BH}} \propto |p - p^*|^\beta$ . Choptuik [1] finds a *universal* critical exponent  $\beta \simeq 0.37$  that is independent of initial wave packet shape. It is thereby conjectured that black holes of infinitesimal mass may be created by this process. For configurations sufficiently close to critical,  $p \simeq p^*$ , a (family-dependent) strong-field region  $\mathcal{R}_k$  exists ( $r$  less than some  $r_k^{\text{max}}$  during the self-interaction) inside of which the scalar field oscillates in a nearly unique fashion. The oscillations are *echoes*, as the field satisfies a remarkable scaling relation

$$\phi(\rho - \Delta, \tau - \Delta) \simeq \phi(\rho, \tau). \quad (1)$$

Here  $\rho$  and  $\tau$  are logarithms of proper (areal) radius  $r$  and central proper time  $T$ :  $\rho = \ln r + \kappa$  and  $\tau = \ln(T^* - T) + \kappa$ , and  $T^*$  is the finite accumulation time of the echoes and  $\kappa$  is a family-specific constant.  $\Delta$  is a *universal* constant found to be  $\simeq 3.4$ , implying that each successive echo appears on spatial and temporal scales a factor  $e^\Delta \simeq 30$  finer than its predecessor. Precisely critical solutions ( $p = p^*$ ) are expected to yield an infinite train of echoes.

In this Letter we report a second example of critical behavior in general relativity, found by studying collapse of axisymmetric *gravitational* wave packets. These spacetimes are physically distinct ( $T^{\mu\nu} = 0$ ), have less symmetry (one instead of two Killing vectors) than spherically symmetric scalar-field collapse, and admit a dynamical degree of freedom of the gravitational field. Elsewhere [2] solutions were computed of select elements of a one-parameter family of gravitational wave packets that demonstrate formation of black holes. Here we examine near-critical solutions and show the existence of critical phenomena similar to that discussed in Ref. [1].

We compute axisymmetric, asymptotically flat vacuum spacetimes using the 3+1 formalism [3], with the maximal time-slicing condition and quasi-isotropic spatial gauge. With 1 dynamical degree of freedom, the line element can be put in the form

$$ds^2 = -\alpha^2 dt^2 + \phi^4 [e^{2\eta/3} (dr + \beta^r dt)^2 + r^2 e^{2\eta/3} (d\theta + \beta^\theta dt)^2 + e^{-4\eta/3} r^2 \sin^2 \theta d\varphi^2], \quad (2)$$

where  $\alpha$  is the lapse function,  $\beta^r$  and  $\beta^\theta$  are shift vector components,  $\phi$  is the conformal factor, and  $\eta$  is the even-parity "dynamical" metric function. Maximal slicing results from the condition  $K^i_i = 0$  on the extrinsic curvature  $K^i_j$ . Numerical solutions of the following equations are computed:

$$\partial_t \hat{\lambda} = \mathcal{D}_\beta[\hat{\lambda}] - \phi^6 (D^r D_r \alpha + 2D^\varphi D_\varphi \alpha) + \alpha \phi^6 (R^r_r + 2R^\varphi_\varphi) + \frac{\hat{K}^r_\theta}{r} \left[ r \partial_r \beta^\theta - \partial_\theta \left( \frac{\beta^r}{r} \right) \right], \quad (3)$$

$$\partial_t \hat{K}^\varphi_\varphi = \mathcal{D}_\beta[\hat{K}^\varphi_\varphi] - \phi^6 D^\varphi D_\varphi \alpha + \alpha \phi^6 R^\varphi_\varphi, \quad (4)$$

$$\partial_t \left( \frac{\hat{K}^r_\theta}{r} \right) = \mathcal{D}_\beta \left[ \frac{\hat{K}^r_\theta}{r} \right] - \frac{1}{r} \phi^6 D^r D_\theta \alpha + \frac{1}{r} \alpha \phi^6 R^r_\theta + (2\hat{\lambda} - 3\hat{K}^\varphi_\varphi) \left[ \partial_\theta \left( \frac{\beta^r}{r} \right) - \alpha \frac{K^r_\theta}{r} \right], \quad (5)$$

$$\partial_t \eta = \beta^r \partial_r \eta + \beta^\theta \partial_\theta \eta + \partial_\theta \beta^\theta - \beta^\theta \cot \theta + \alpha \lambda, \quad (6)$$

$$\Delta_f^{(3)} \psi = -\frac{1}{4} \psi \left( \Delta_f^{(2)} \eta + \frac{1}{2} \psi^{-8} e^{-2\eta} \hat{K}^i_j \hat{K}^j_i \right), \quad (7)$$

$$\Delta_f^{(3)} (\alpha \psi) = -\frac{1}{4} \alpha \psi \left( \Delta_f^{(2)} \eta - \frac{7}{2} A^2 K^i_j K^j_i \right), \quad (8)$$

$$r \partial_r \left( \frac{\beta^r}{r} \right) - \partial_\theta \beta^\theta = \alpha (2\lambda - 3K^\varphi_\varphi), \quad (9)$$

$$r \partial_r \beta^\theta + \partial_\theta \left( \frac{\beta^r}{r} \right) = 2\alpha \frac{K^r_\theta}{r}, \quad (10)$$

where

$$K^i_j K^j_i = 2\lambda^2 - 6\lambda K^\varphi_\varphi + 6(K^\varphi_\varphi)^2 + 2 \left( \frac{K^r_\theta}{r} \right)^2,$$

and where the operator  $\mathcal{D}_\beta$  is defined by

$$\mathcal{D}_\beta[u] = \frac{1}{r^2} \partial_r [r^2 \beta^r u] + \frac{1}{\sin \theta} \partial_\theta [\sin \theta \beta^\theta u].$$

In these equations we define  $\lambda = K^r_r + 2K^\varphi_\varphi$ ,  $\hat{K}^i_j = \phi^6 K^i_j$ , and  $D_k$  is the spatial covariant derivative,  $R^i_j$  is the spatial Ricci tensor,  $A = \phi^2 e^{\eta/3}$ ,  $B = \phi^2 e^{-2\eta/3}$ ,  $\psi = B^{1/2}$ , and  $\Delta_f^{(3)}$  and  $\Delta_f^{(2)}$  are the three- and two-dimensional, flat-space Laplacians, respectively. Analytic properties of this gauge have been explored in Refs. [4–7]. Portions of the finite difference method are described elsewhere [4, 5].

Various quasilocal mass indicators (Brill, Hawking, and Arnowitt-Deser-Misner (ADM) [4]) are used as diagnostics of the fidelity of the simulations. We locate [2, 8] marginally outer-trapped surfaces when they form. Estimates of asymptotic gravitational wave forms are extracted at finite radii by various complementary means [7, 9, 10].

We choose Cauchy data by fixing the freely specifiable fields,  $\eta$  and  $K^r_\theta$ , to have the form of a *linear* ingoing gravitational wave packet possessing quadrupolar ( $\ell = 2$ ) angular dependence. The general linear  $\ell = 2$  solution [11] has been expressed in quasi-isotropic gauge in Ref. [7]. This solution is determined by a quadrupole moment  $I(v)$  of arbitrary profile, its derivatives,  $I^{(1)}(v) \equiv dI(v)/dv$  and  $I^{(2)}(v)$ , and its integrals,  $I^{(-1)}(v) \equiv \int^v dv' I(v')$  and  $I^{(-2)}(v)$ . As functions of advanced time  $v$ ,  $\eta$  and  $K^r_\theta$  are

$$\eta = \left( \frac{I^{(2)}}{r} - 2 \frac{I^{(1)}}{r^2} \right) \sin^2 \theta,$$

$$\frac{K^r_\theta}{r} = \left( \frac{I^{(2)}}{r^2} - 3 \frac{I^{(1)}}{r^3} + 6 \frac{I}{r^4} - 6 \frac{I^{(-1)}}{r^5} \right) \sin 2\theta.$$

However, wave packets of finite amplitude confined within a finite volume generate nonlinear Cauchy data. Accordingly, we solve the exact Hamiltonian and momentum constraints for  $\phi$ ,  $\lambda$ , and  $K^\varphi_\varphi$ , subject to the choice above of  $\eta$  and  $K^r_\theta$ . The nearly linear Cauchy data are found still to generate ingoing solutions, which are dominated by  $\ell = 2$  angular dependence. Centered initially about a radius  $r_0$  and confined to a width  $L \ll r_0$ , nearly linear wave packets have ADM mass  $M_p \lesssim M_p^{\text{linear}}$ , differing by a fraction of  $\mathcal{O}(M_p/r_0)$ .

We compute solutions that lie within a one-parameter family  $\mathcal{S}[a]$  generated from initial  $\ell = 2$  wave packets with polynomial radial dependence of the form  $I^{(-2)}(v) = a \kappa_p L^5 [1 - (v/L)^2]^6$  for  $|v| = |r - r_0| < L$  at  $t = 0$ . Here,  $a$  is an amplitude parameter,  $L$  is a width parameter, and  $\kappa_p = \frac{1}{12288} \sqrt{143/\pi}$ . In the limit  $a \rightarrow 0$ , the mass of the wave packet is  $M_p^{\text{linear}} = a^2 L / (2\pi)$ . A useful alternative strength parameter is  $\Theta(a) = 2\pi M_p / L \simeq a^2$ .

As shown before [2], a wave packet with  $\Theta \ll 1$  only weakly self-interacts, escaping to infinity virtually unaffected. Conversely, a black hole forms in an evolution where  $\Theta \gtrsim 1$ , with  $M_{\text{BH}} \rightarrow M_p$  as  $\Theta \rightarrow \infty$ . We find the critical value along the sequence to be  $\Theta^* \simeq 0.80$  ( $a^* \simeq 0.93$ ). Figure 1 illustrates the behavior of two near-critical solutions lying on either side of  $\Theta^*$  by showing the time dependence of the central value of the lapse function.

Like Choptuik [1], in the supercritical regime ( $\mathcal{S}[a \gtrsim a^*]$ ) we observe that black-hole mass,  $M_{\text{BH}}$ , is well described by a power law

$$M_{\text{BH}} \simeq C(a - a^*)^\beta. \quad (11)$$

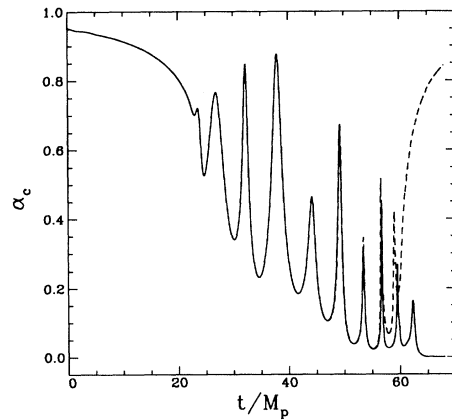


FIG. 1. Near-critical evolution illustrated by the time dependence of the central value of the lapse function. Supercritical (solid) and subcritical (dashed) solutions are shown for amplitudes  $a = 0.9303$  and  $a = 0.9302$ , respectively. A number of oscillations occur during the period of strong self-interaction. The solutions diverge only in the last several oscillations, followed by exponential collapse of  $\alpha_c$  in the supercritical case and  $\alpha_c \rightarrow 1$  in the subcritical case.

Quite remarkably, the critical exponent value we obtain,  $\beta \simeq 0.37$ , for gravitational wave collapse is indistinguishable from that seen in scalar-field collapse. Figure 2 shows the power-law behavior of black-hole mass found in a sequence of simulations.

Determining  $M_{\text{BH}}$  is made difficult by the hole's initial asymmetry, which leads to emission of quasinormal mode (QNM) radiation as the black hole rings down [2]. By  $M_{\text{BH}}$  we mean the mass  $\sqrt{\mathcal{A}_{\text{ah}}/16\pi}$  computed from the area of the apparent horizon  $\mathcal{A}_{\text{ah}}$  at a time  $\Delta t = 2\pi/\omega_1^{\ell=2}$  (where  $\omega_1^{\ell=2}$  is the real part of the lowest-order  $\ell = 2$  QNM frequency) after the apparent horizon first appears. In most cases extracted  $\ell = 2$  and  $\ell = 4$  wave forms are fit [2] by their respective lowest-order QNM's to provide redundant estimates of  $M_{\text{BH}}$ .

With our present method and accessible range of resolution we are only able to find black holes with masses  $M_{\text{BH}} \gtrsim 0.2M_p$ . Significantly, the scaling law (11) holds even in this range, similar to the scalar-field case [1]. Masses  $M_{\text{BH}}(a)$  are obtained from a sequence of simulations with 290 radial and 16 angular zones and consistently chosen grid properties. The data are least squares fitted by the functional form (11) to determine  $a^*$ ,  $C$ , and  $\beta$ , yielding a formal value  $\beta = 0.369$  of the critical exponent. A fit to  $M_{\text{BH}}$  versus  $\Theta$  instead yields a formal value  $\beta = 0.361$ . The critical point locations derived from fitting are  $\Theta^* = 0.799$  and  $a^* = 0.928$ , which correspond to each other to about 1 part in  $10^{-4}$ , but differ by  $\simeq 2 \times 10^{-3}$  at this numerical resolution from the critical point location  $a^* = 0.9302$  determined by binary search of the solution space. Similarly, results from several numerical surveys indicate  $\beta$  to be dependent on grid properties and resolution. At present, we estimate

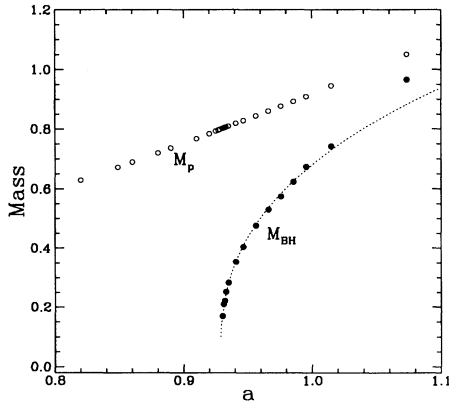


FIG. 2. Critical behavior of black-hole mass. Black-hole masses  $M_{\text{BH}}$  derived from a sequence of simulations are plotted (filled circles) as a function of initial wave packet amplitude. The quasilocal (Brill) masses  $M_p$  of the wave packets are shown (open circles) for comparison. The dotted curve represents the best-fit power law  $M_{\text{BH}} = C(a - a^*)^\beta$  with values  $a^* = 0.928$ ,  $C = 1.750$ , and  $\beta = 0.369$ . Wave packet width  $L = 2\pi$  is chosen to normalize the mass scale.

the true value of  $\beta$  to lie in the range 0.35 to 0.38, a span encompassing the range found [1] for scalar-field collapse.

We observe tentative evidence for self-similar scaling of the gravitational field in the strong-field region  $\mathcal{R}$ . As Fig. 1 indicates, the central value of the lapse,  $\alpha_c$ , oscillates in the strong-field regime. At times coincident with every other maximum of  $\alpha_c$ ,  $t = t_n(\alpha_c^{\text{max}})$ , we observe that a new complete oscillation, or echo, appears in  $\mathcal{R}$ . Variations in resolution indicate these features are robust. For example, the same features appear in models that differ by a factor of 1.5 in both angular and radial discretization scales. As Fig. 3 illustrates, the radial profiles of the echoes in  $\eta$  exhibit approximate scaling in  $\rho = \ln r$ :

$$\eta(\rho - \Delta, t_n) \simeq \eta(\rho, t_{n+1}), \quad (12)$$

with a single value of  $\Delta$  associated with the self-similarity. The scaling constant  $\Delta \simeq 0.6$  implies a radial scale ratio  $e^\Delta \simeq 1.8$  which differs considerably from the

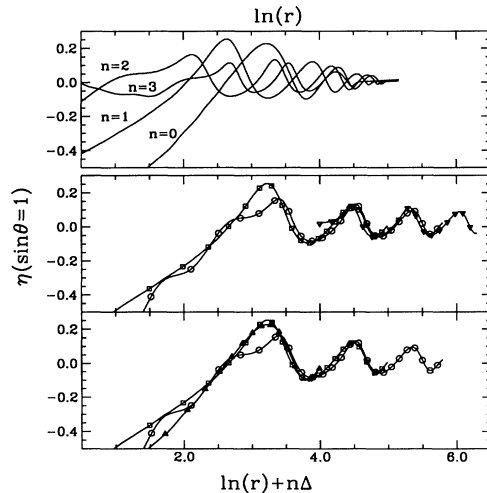


FIG. 3. Scaling property exhibited in a near-critical solution. Data are from a subcritical numerical solution with a critical separation  $(a^* - a)/a^* < 10^{-4}$  determined by binary search. Radial profiles of the metric function  $\eta$ , restricted to the symmetry plane  $\theta = \pi/2$ , are plotted at four different times corresponding to alternate maxima of the oscillations in  $\alpha_c$  (see Fig. 1 and text). The upper panel depicts all four radial profiles (labeled sequentially  $n = 0 - 3$ ) plotted vs  $\rho = \ln r$ . The two lower panels illustrate the scaling property of the echoes by overlapping profiles that are shifted by  $\rho \rightarrow \rho' = \rho + n\Delta$  with an empirically determined scaling constant of  $\Delta \simeq 0.6$ . To enhance clarity, only profiles  $n = 0, 1, 2$  are plotted in the bottom panel and only  $n = 1, 2, 3$  in the middle panel. The outer, nonscaling edge of each profile is truncated in the two lower panels as is the inner edge of the  $n = 3$  profile (at which point the subcritical configuration has begun to escape). The radial resolution of these profiles is indicated by plotting the location of every tenth grid point. These locations are denoted by triangles ( $n = 0$ ), squares ( $n = 1$ ), circles ( $n = 2$ ), and inverted triangles ( $n = 3$ ).

corresponding value of  $e^\Delta \simeq 30$  ( $\Delta \simeq 3.4$ ) in scalar-field collapse.

We conjecture that in the precisely critical case ( $a = a^*$ ) the gravitational field in  $\mathcal{R}$  approaches a unique two-dimensional solution as  $r \rightarrow 0$ . Its angular properties have not been ascertained but we do observe a distinct train of oscillations with  $\ell = 4$  angular dependence. This  $\ell = 4$  dependence is primarily created by the nonlinearities within  $\mathcal{R}$  and is distinct from the small component of this multipole present in the initial wave packet. Thus, a multipole analysis may also serve as a useful diagnostic of the self-similarity of the echoing.

How close is the association between the critical behavior in these spacetimes and standard critical phenomena? The appearance of black holes in only those solutions with  $a > a^*$ , and the reasonable conjecture that a hole of infinitesimal mass appears at  $a = a^*$ , suggests that  $M_{\text{BH}}$  plays the role of *order parameter* for these critical phenomena. It is interesting to note that the critical exponent associated with this order parameter lies in a range typically observed for  $\beta$  in other critical systems. Choptuik [1] has shown that details inherent in the original data are “washed out” within  $\mathcal{R}$  in near-critical evolutions. Information may be steadily lost with each echo as  $r \rightarrow 0$  and  $T \rightarrow T^*$  and the rate of loss per echo may depend on the value of  $\Delta$ . An analog of the correlation length  $\xi$  in statistical systems may be the ratio of the radii of the outer edge of the scaling region,  $r_{\text{max}}$ , and the inner edge,  $r_n$ , of the innermost echo: i.e.,  $\xi \sim r_{\text{max}}/r_n \sim e^{n\Delta}$ . As  $a \rightarrow a^*$  an ever-larger region (in terms of the scale  $r_n$ ) becomes “correlated” with self-similar echoes and  $\xi \rightarrow \infty$ .

We thank M. Choptuik for discussions and for informing us of his results prior to publication. This research was supported in part by NSF Grants No. AST 90-15451 at Cornell University and No. PHY 90-01645 and No. PHY 90-57865 at the University of North Carolina. A.M.A. gratefully acknowledges the support of the NSF Division of Advanced Scientific Computing. C.R.E. thanks the Sloan Foundation for research support. Computations were performed at the North Carolina Supercomputing Center and at the NSF National Center for Supercomputing Applications.

- (a) Also at Center for Theory and Simulation in Science and Engineering, Cornell University, Ithaca, NY 14853.
- [1] M. W. Choptuik, Phys. Rev. Lett. **70**, 9 (1993).
  - [2] A. M. Abrahams and C. R. Evans, Phys. Rev. D **46**, R4117 (1992).
  - [3] J. W. York, in *Sources of Gravitational Radiation*, edited by L. Smarr (Cambridge Univ. Press, Cambridge, 1979).
  - [4] C. R. Evans, Ph.D. thesis, University of Texas at Austin, 1984 (unpublished).
  - [5] C. R. Evans, in *Dynamical Spacetimes and Numerical Relativity*, edited by J. Centrella (Cambridge Univ. Press, Cambridge, 1986).
  - [6] J. M. Bardeen and T. Piran, Phys. Rep. **96**, 205 (1983).
  - [7] A. M. Abrahams and C. R. Evans, Phys. Rev. D **37**, 318 (1988).
  - [8] P. G. Dykema, Ph.D. thesis, University of Texas at Austin, 1980 (unpublished).
  - [9] A. M. Abrahams and C. R. Evans, Phys. Rev. D **42**, 2585 (1990).
  - [10] A. M. Abrahams and C. R. Evans (to be published).
  - [11] S. A. Teukolsky, Phys. Rev. D **26**, 745 (1982).